IOP Conf. Series: Earth and Environmental Science **35** (2016) 012009 doi:10.1088/1755-1315/35/1/012009

Estimation of friction velocity from the wind-wave spectrum at extremely high wind speeds

N Takagaki[1], S Komori[1] and N Suzuki[2]

[1]Department of Mechanical Engineering and Science and Advanced Research Institute of Fluid Science and Engineering, Kyoto University, Kyoto 615-8540, Japan
[2]Department of Mechanical Engineering, Kinki University, Osaka 577-8502, Japan

komori@mech.kyoto-u.ac.jp

Abstract. The equilibrium range of wind-waves at normal and extremely high wind speeds was investigated experimentally using a high-speed wind-wave tank together with field measurements at normal wind speeds. Water level fluctuations at normal and extremely high wind speeds were measured with resistance-type wave gauges, and the wind-wave spectrum and significant phase velocity were calculated. The equilibrium range constant was estimated from the wind-wave spectrum and showed the strong relationship with inverse wave age at normal and extremely high wind speeds. Using the strong relation between the equilibrium range constant and inverse wave age, a new method for estimating the wind speed at 10-m height (U_{10}) and friction velocity (u^*) was proposed. The results suggest that U_{10} and u^* can be estimated from wave measurements alone at extremely high wind speeds in oceans under tropical cyclones.

1. Introduction

It is of great importance to predict the development and decay of tropical cyclones accurately in order to minimize loss of life and property, since tropical cyclones can wreak catastrophic damage to a local society by generating gales, storm surges, and heavy rain. Reliable predictions of tropical cyclone intensity require accurate estimates of momentum and heat transfer across the sea surface. An important goal in constructing a reliable model to forecast the decay or development of a tropical cyclone is how to accurately estimate momentum transfer rate across the air-sea interface in stormy conditions. Such an estimate requires an accurate drag coefficient (C_D) model against wind speed at z = 10 m above the sea surface (U_{10}). The sea surface wind shear stress (τ) is expressed as:

$$\tau = \rho u^{*2} = \rho C_D U_{10}^2, \tag{1}$$

where ρ is the density of air and u^* is the air friction velocity.

Recent field measurements [1] made by a Global Positioning System dropsonde in a tropical cyclone showed that C_D decreases with increasing U_{10} at extremely high wind speeds of $U_{10} \gtrsim 35$ m/s, whereas previous field [2] and laboratory measurements [3] suggested that C_D increases with increasing U_{10} also at extremely high wind speeds. Recent laboratory data [4, 5] show almost constant values of C_D at extremely high wind speeds of U_{10} = 35 ~ 68 m/s; data reported by Takagaki *et al*. [5] were measured directly by an eddy correlation method [see 6, 7] using a phase Doppler anemometer (PDA). Thus, the trend of C_D at extremely high wind speeds remains controversial: increasing, decreasing, or constant

with U_{10}. For field measurements, very expensive dropsondes and aircraft are used to measure wind speed in and under tropical cyclones. These dropsondes have revealed significant new evidence for momentum transfer across the sea surface under tropical cyclones [e.g., 1, 8, and 9]. However, it is prohibitively expensive to use dropsondes and aircraft to observe entire tropical cyclones and forecast weather. Therefore, alternative simple instruments and techniques for measuring U_{10} and C_D under tropical cyclones are needed.

At normal wind speeds of $U_{10} < 35$ m/s in the absence of tropical cyclones, spaceborne radar observations are generally used to estimate wind speeds near the sea surface by exploiting the strong relationship between the small-scale surface structure on wind-waves and the relative backscattering intensity of radar. For example, previous studies [10–13] developed several methods to estimate U_{10} or u^* from wind-wave data. The mean square slope of the sea surface [10, 11] or the equilibrium range of the wind-wave spectrum [12, 13], which gives wind-wave energy level, are used to estimate wind speeds at $U_{10} < 20$ m/s. And Donelan *et al*. [4] demonstrated that general 5.3 GHz (C band) microwave radar observations are not applicable to observations under tropical cyclones. However, if an equilibrium range exists at extremely high wind speeds, simple physical-based instruments and techniques for measuring U_{10} and C_D under tropical cyclones might be feasible.

The purpose of this study is, therefore, to clarify the wind-wave spectral shape, then to clarify the existence of an equilibrium range of wind-waves at extremely high wind speeds, and to develop a model for calculating the dimensionless equilibrium range constant. By using the model for the dimensionless equilibrium range constant, we propose a method to estimate U_{10} (or u^*) and quantify the error of this method.

2. Experiments

2.1. Laboratory experiment

The high-speed wind-wave tank [5, 14, and 15] with a glass test section 15.0 m long, 0.8 m wide, and 1.6 m high was used. Wind-waves were driven in the water tank by wind at $U_{10} = 7 - 68$ m/s. Wind velocity and water-level fluctuations were measured at a fetch of $x = 6.5$ m from the edge ($x = 0$ m) of the entrance slope plate.

A laser Doppler anemometer (Dantec LDA) and phase Doppler anemometer (Dantec PDA) were used to measure the wind-velocity fluctuations. And the shear stress at the interface was estimated by an eddy correlation method [5].

Water level fluctuations were measured using resistance-type wave gauges (Kenek CHT4-HR60BNC). The resistance wire was placed in the water, and the electrical resistance due to the instantaneous water level was recorded at 500 Hz and 600 s on a digital recorder (Sony EX-UT10). The energy of the wind-waves (E) was estimated by integrating the spectrum of water level fluctuations against the frequency (f) and the significant frequency of wind-waves (f_m) was defined as the peak frequency of the spectrum.

To determine whether the dispersed droplets and entrained bubbles from the intensively breaking wind-waves caused problems for the wave gauge, we photographed the surface of breaking wind-waves with a high-speed camera (DANTEC NanoSense Mk3) synchronized to the gauge. The gauge was mounted at 0.02 m from the glass side wall of the wind-wave tank. The high-speed camera was operated at a speed of 100 frames per second to capture the surface of breaking wind-waves at the side wall of the tank. The sampling time was 20 s. The spatial resolution of a digital CMOS camera was 1280 × 1024 pixels for the imaging area of 130 mm × 100 mm ($U_{10} < 30$ m/s) and 260 mm × 200 mm ($U_{10} \gtrsim 30$ m/s). The instantaneous surface elevation from the still water level was estimated from the image by eye, because it was difficult to calculate it using an analytical program owing to the intensive breaking of wind-waves.

For measuring both the wave length (L_S) and phase velocity (C_P) of significant wind-waves, another wave gauge was fixed downstream at $\Delta x = 0.02$ m for $U_{10} < 30$ m/s and at $\Delta x = 0.19$ m for $U_{10} \gtrsim 30$ m/s. The values of C_P were estimated using the cospectrum method [e.g., 16].

2.2. Field experiment

We analysed wind and wave data recorded on an observation tower operated by the Shirahama Oceanographic Observatory, Disaster Prevention Research Institute (DPRI), Kyoto University, Japan. The tower is located at 33.4232°N and 135.1958°E in Tanabe Bay, Wakayama, Japan. The distance from the tower to the nearest coastline is about 1 km and the water depth at the tower is 30 m. The data period was from 1 January 2005 to 31 December 2009. A sonic anemometer was installed on the tower at a height of 20 m above the mean sea surface. The two horizontal and one vertical components of wind velocity were recorded at a sampling frequency of 10 Hz. The U_{10}, u^*, and wind-wave spectrum were calculated according to the methods described in Takagaki *et al*. [5].

3. Results and discussion

Figure 1 shows the wind-wave spectra at normal (U_{10} = 17 m/s) and extremely high (U_{10} = 48, 67 m/s) wind speeds obtained by wave-gauge measurements. The spectra and frequencies are normalized by the total energy (E) and significant frequency (f_m) of the wind-waves. Three solid lines showing slopes of –3, –4, and –5 at frequencies higher than f_m are described in figure 1. At normal wind speeds, the present slope at frequencies higher than f_m corresponds to the –4 slope instead of the –3 and –5 slopes (figure 1a). The –5 slope, proposed by Phillips [17], has been used in many models for wind-wave spectra [e.g., 18, 19]. The –4 slope, proposed by Toba [20] in relation to Toba's 3/2 law [21], indicates the local equilibrium between wind shear and wind-waves. It has been shown to be suitable for representing the wind-wave spectra for oceans and wind-wave tanks at normal wind speeds of $U_{10} < 35$ m/s [e.g., 22–25]. However, at extremely high wind speeds of $U_{10} \gtrsim 35$ m/s, the magnitude of the slope at frequencies higher than f_m is unknown. In figure 1b and 1c, the slope at extremely high wind speeds corresponds to the –4 slope within the region immediately after the spectral peak. This means that in the region immediately after spectral peak, a spectral energy balance mechanism [e.g., 26], similar to that at normal wind speeds, might also operate at extremely high wind speeds. On the other hand, the spectral slope becomes gentler in the region at $f > 5$ Hz. Although the gentler slope at $f > 5$ Hz may be due to measurement error or enhancement of the energy of wind-waves by the particular breaking of significant wind-waves, we cannot investigate the phenomenon here because of a lack of information on the development of wind-waves at extremely high wind speeds. Thus, the spectra at $f > 5$ Hz were eliminated from figure 1b and 1c.

Generally, the wind-wave spectral form at a slope of –4 (see figure 1) is shows as:

$$S(f) = \alpha_T (2\pi)^{-3} g u^* f^{-4} \tag{2}$$

or

$$S(f) = \alpha_D (2\pi)^{-4} g^2 f_m^{-1} f^{-4}, \tag{3}$$

where g is the acceleration due to gravity and u^* is air-friction velocity. In addition, equilibrium range constants α_T and α_D are the so-called Toba's constant and Donelan's constant, respectively. Although Toba's constant α_T was assumed to be a constant value [e.g., 22], many recent studies suggest that its value depends on inverse wave age (U_{10}/C_P) [e.g., 12, 25, and 27]. In addition, Donelan's form shown as equation (3) is suitable for estimating U_{10} (or u^*) from the wind-wave spectrum, because the form

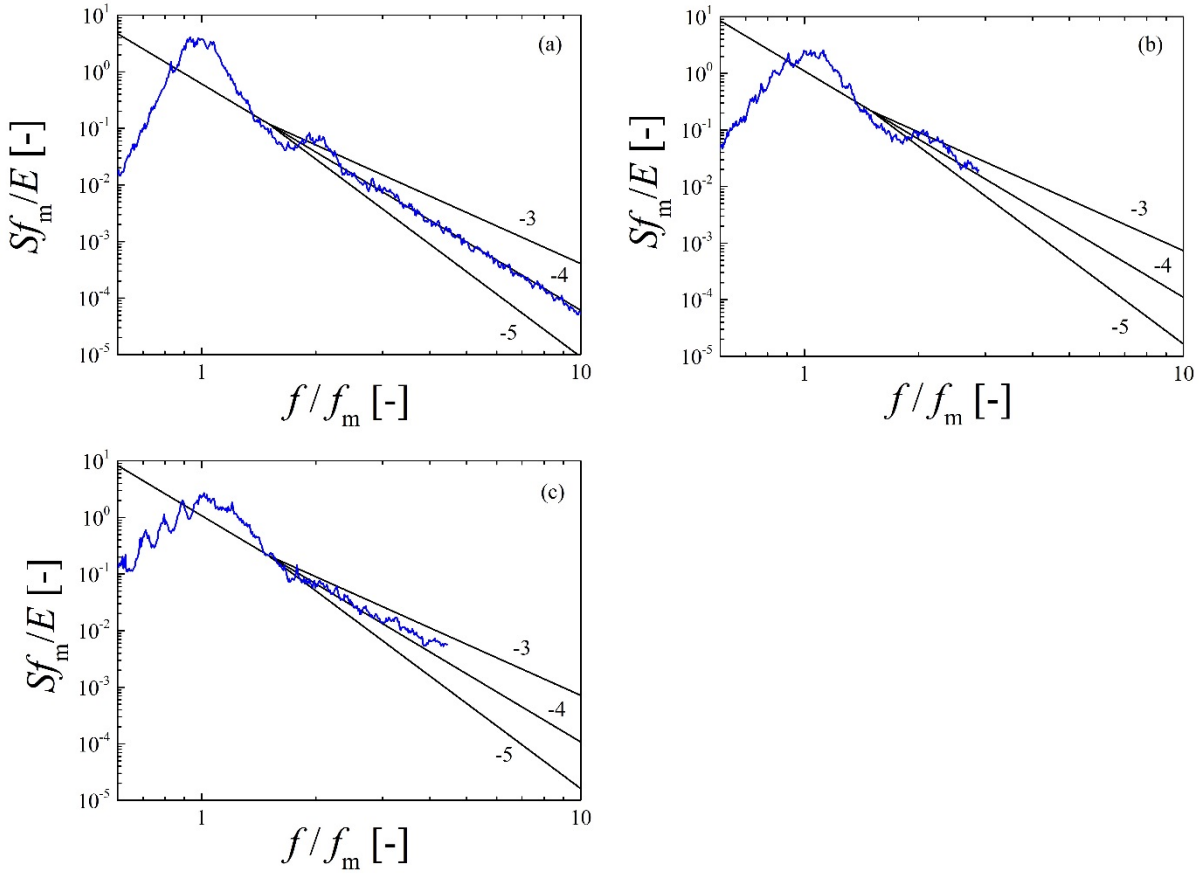

Figure 1. Wind-wave spectra at (a) normal wind speeds (U_{10} = 17 m/s), (b) extremely high wind speeds (U_{10} = 48 m/s) and (c) extremely high wind speeds (U_{10} = 67 m/s). Spectra (S) and frequency (f) are normalized by the total energy (E) and significant frequency (f_m) of wind-waves. Spectra at extremely high wind speeds (U_{10} = 48, 67 m/s) are described under f = 5 Hz by rejecting impingement effects of droplets and bubbles on water-level measurements. Three solid lines (upper, middle, and lower) are the slopes of –3, –4, and –5.

does not include a wind speed parameter directly. Therefore, in the present study, we chose Donelan's form (equation 3) and Donelan's constant α_D to develop a model of the equilibrium range constant and propose an estimation method for U_{10} (or u^*).

Figure 2 shows the relationship between the dimensionless equilibrium range constant (αD), showing energy levels within the equilibrium range, and inverse wave age (U10/CP). The values of αD were estimated from the wind-wave spectra in the equilibrium range [e.g., 12, 25, and 27]. The present laboratory/field data at normal wind speeds of U_{10} < 35 m/s increase monotonically with increasing U_{10}/C_P, although the present field data are somewhat scattered and have lesser values than previous field studies [23 – 25, 28, and 29]. On the other hand, present laboratory data at extremely high wind speeds of $U_{10} \gtrsim 35$ m/s are plotted on a smaller range of U_{10}/C_P, and take constant values of both α_D and U_{10}/C_P, ($\alpha_D \sim 0.05$ at $U_{10}/C_P \sim 30$). This trend of taking constant values is one of the reasons for the collapse of the local equilibrium of wind and wind-waves [5] at extremely high wind speeds. Then, from this trend of α_D at extremely high wind speeds, we can produce the best-fit curve:

$$\alpha_D = 0.00136 \left(\frac{U_{10}}{C_p}\right)^{1.0} \quad (5)$$

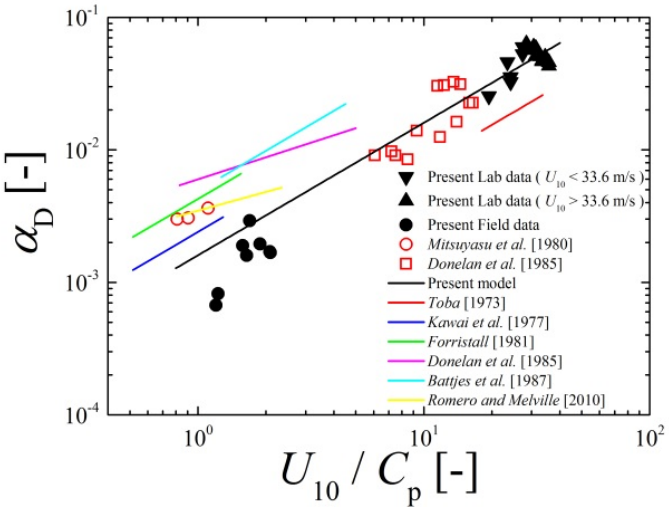

Figure 2. Relationship between the dimensionless equilibrium range constant (α_D), showing energy levels within the equilibrium range, and inverse wave age (U_{10}/C_P). The values of α_D are calculated from α_T [20, 24, 25, and 28–30] by $\alpha_D = \alpha_T (U_{10}/C_P) C_D^{1/2}$, derived from equations (2), (3), and the assumption of deep-sea waves, under the constant drag coefficient (C_D) of 0.0015. Values of α_D [30] at $U_{10}/C_P > 0.73$ are accepted here because of the limitation of the fully-developed wind-waves proposed by [31]. The solid black curve shows the best-fit against the values of α_D in present and previous [23, 30] laboratory/field studies. For Donelan *et al*. [23], the laboratory and field data are shown as open square plots and pink curve, respectively.

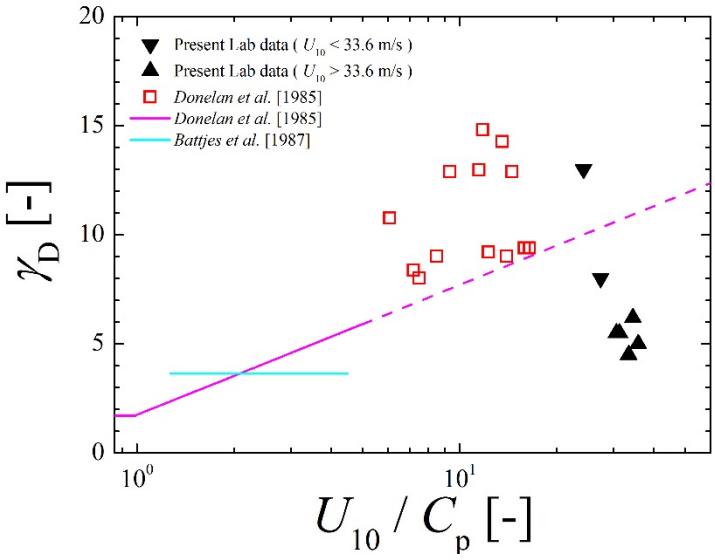

Figure 3. Relationship between the dimensionless peak enhancement factor (γ_D) and inverse wave age (U_{10}/C_P). The γ_D is evaluated according to $S(f) = \alpha_D (2\pi)^{-4} g^2 f_m^{-1} f^{-4} \exp\left(-\left(\frac{f}{fm}\right)^4\right) \gamma_D^{\Gamma}$ proposed by Donelan *et al*. [23]. The dotted curve shows the extrapolated curve of Donelan *et al*. [23]. For Donelan *et al*. [23], the laboratory and field data are shown as open square plots and pink curve, respectively.

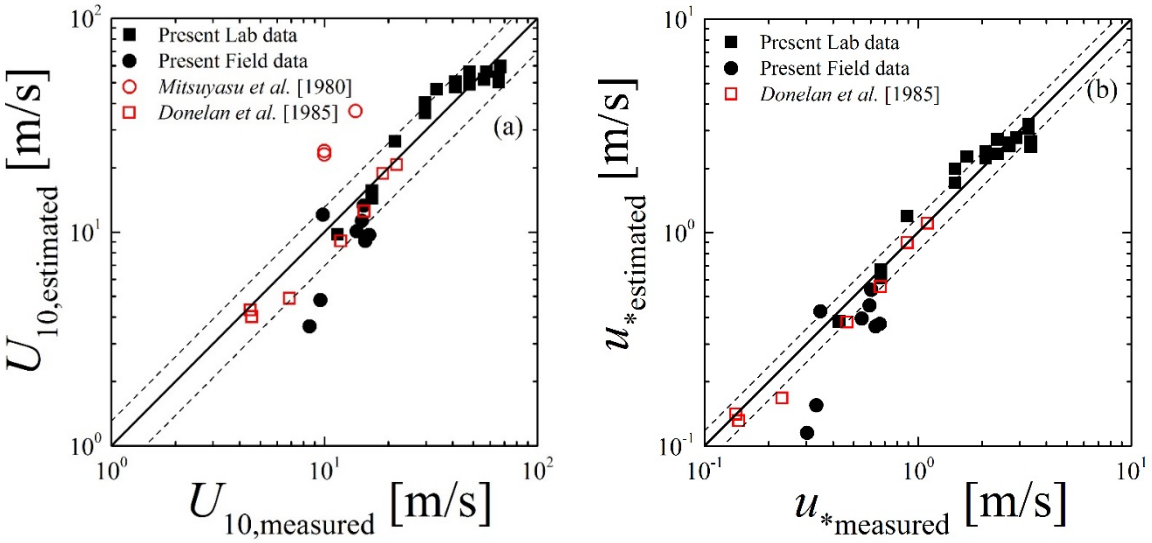

Figure 4. Relationship between measured and estimated values of (a) 10 m-height wind speed (U_{10}) and (b) air friction velocity. Data [30] are shown only in (a), because the article provides values of U_{10}. Upper and lower dashed lines in figure 4(a) and (b) show the upper and lower limitations estimated from the mean absolute percent error (30% and 18%, respectively).

from the present laboratory/field data, previous laboratory data [23], and previous field data [30] over a wide range of U_{10}/C_P = 0.83 ~ 36 and U_{10} = 4.5 ~ 68 m/s (see black curve in figure 2). The curve of equation (5) seems to be a good fit for data at normal wind speeds as well as data at extremely high wind speeds, with a correlation coefficient of R^2 = 0.9164. In addition, because the maximum wavelength of significant wind-waves (L_S) in the wind-wave tank is about 1.9 m at the highest wind speed (U_{10} = 68 m/s), the ratio of the water depth (D = 0.8 m) to wavelength (D/L_S) is nearly 0.5, which is a strict criterion for deep-sea waves [see 32]. This means that the wind-waves in our wind-wave tank could be regarded as almost deep-sea waves under all laboratory conditions in the present study, and that the relationship between α_D and U_{10}/C_P (figure 2) is not affected by water depth. Therefore, when α_D is measured along with C_P under tropical cyclones in real oceans, it might be possible to estimate U_{10} using equation (5). Figure 3 shows the relationship between the peak enhancement factor (γ_D) and inverse wave age (U_{10}/C_p). Although at normal wind speeds of U_{10} < 35 m/s, the present laboratory data increase monotonically with increasing U_{10}/C_p, present laboratory data at extremely high wind speeds of $U_{10} \gtrsim$ 35 m/s decrease rapidly with increasing U_{10}/C_p. This reduction of the peak enhancement factor at extremely high wind speeds indicates that the large-scale geometry corresponding to the significant waves is broken by intensive wind shear, and the reduction is the main reason for the collapse of the local equilibrium of wind and wind-waves [5].

Figure 4 shows the relationship between measured and estimated values of 10-m height wind speed (U_{10}) and air friction velocity (u^*). Estimated values of U_{10} were calculated from the values of α_D and C_P in equation (5). In addition, estimated values of u^* were calculated from estimated U_{10} and an empirical relation [5] shown as:

$$E^* = c f_m^{*-3}, \tag{6}$$

where E^* (= E/z_0^2) is the wave energy E normalized by the roughness length z_0, f_m^* (=$f_m(z_0/g)^{1/2}$) is the normalized significant frequency of wind-waves, c = 1.2×10^{-3}, and Equation (6) means that z_0 and C_D are uniquely determined by the shape of wind-waves at both normal and extremely high wind speeds.

The correlation coefficients are $R^2 = 0.924$ for U_{10} and $R^2 = 0.966$ for u^*, and this means that the values of U_{10} and u^* are fairly accurate despite their estimation from wave measurements alone, without any wind measurements, at extremely high wind speeds in oceans under tropical cyclones.

In summary, by wave measurements in oceans under tropical cyclones, U_{10} can be estimated as:

$$U_{10} = \frac{\alpha_D}{0.00136} \frac{g}{2\pi f_m}, \tag{7}$$

which is derived from equation (5), the dispersion relation for deep-sea waves ($2\pi f_m^2 = g/L_S$), and $C_P = f_m L_S$. The friction velocity (u^*) can be estimated as:

$$u^* = \kappa U_{10} \left(\ln \frac{10}{z_0}\right)^{-1} = \kappa \left(\frac{\alpha_D}{0.00136} \frac{g}{2\pi f_m}\right) \left(\ln \frac{10}{c^{-2} E^2 f_m^6 g^{-3}}\right)^{-1}, \tag{8}$$

where κ (=0.4) is the von Kármán constant, and equation (8) is derived from equations (6) and (7) and the log-law under neutral conditions. Equations (7) and (8) show that U_{10} and u^* can be estimated from wave measurements alone, because α_D can be estimated by equation (3) and E can also be estimated by integrating the spectrum of water level fluctuations. We expect that equations (7) and (8) will support fundamental ocean studies and improve the precision of weather forecasting under tropical cyclones.

Acknowledgments
This work was supported by the Ministry of Education, Science, Sports and Culture, Grant-in Aid (25249013, 24360069). We gratefully acknowledge Y. Muto, Y. Baba, S. Serizawa and T. Kubo of Shirahama Oceanographic Observatory, Disaster Prevention Research Institute, Kyoto University, for providing us with the data observed at Tanabe-Nakashima oceanographic observation tower.

References

[1] Powell M D *et al* 2003 *Nature* **422** 279
[2] Hawkins H F and Rubsam D T 1968 *Mon. Wea. Rev.* **96** 617
[3] Kunishi H and Imasato N 1966 *Disaster Prevention Res. Inst. Ann.* **9** 1
[4] Donelan M A *et al* 2004 *Geophys. Res. Lett.* **31** doi:10.1029/2004GL019460
[5] Takagaki N *et al* 2012 *Geophys. Res. Lett.* **39** doi:10.1029/2012GL053988
[6] Komori S *et al* 1993 *J. Fluid Mech.* **249** 161
[7] Takagaki N and Komori S 2007 *J. Geophys. Res.* **112** doi:10.1029/2006JC003752
[8] Holthuijsen L H *et al* 2012 *J. Geophys. Res.* **117** doi:10.1029/2012JC007983
[9] Richter D H and Stern D P 2014 *Geophys. Res. Lett.* **41** doi: 10.1002/2014GL059746.
[10] Young I R 1993 *J. Geophys. Res.* **98** 20275
[11] Zhao D and Toba Y 2003 *J. Oceanogr. Soc. Japan* **59** 235
[12] García-Nava H *et al* 2012 *J. Geophys. Res.* **117** doi:10.1029/2011JC007833
[13] Thomson J *et al* 2013 *J. Geophys. Res.* **118** doi:10.1002/2013JC008837
[14] Iwano K *et al* 2013 *Tellus* B **65** 21341
[15] Krall K E and Jähne B 2014 *Ocean Sci.* **10** 257
[16] Mitsuyasu H *et al* 1979 *J. Fluid Mech.* **92** 731
[17] Phillips M 1958 *J. Fluid Mech.* **4** 426
[18] Pierson W J and Moskowitz L 1964 *J. Geophys. Res.* **69** 5181
[19] Hasselmann K *et al* 1973 *Erganzugsh. Dtsch. Hydrogr. Z.* **12** 1-95
[20] Toba Y 1973 *J. Oceanogr. Soc. Japan* **29** 209
[21] Toba Y 1972 *J. Oceanogr. Soc. Japan* **28** 109
[22] Phillips O M 1985 *J. Fluid Mech.* **156** 505
[23] Donelan M A *et al* 1985 *Philos. Trans. R. Soc. London* A **315** 509

[24] Battjes J A *et al* 1987 *J. Phys. Oceanogr.* **17** 1288
[25] Romero L and Melville W K 2010 *J. Phys. Oceanogr.* **40** 441
[26] Holthuijsen L H 2007 *Waves in Oceanic and Coastal Waters* (Cambridge: Cambridge Univ. Press)
[27] Resio D T *et al* 2004 *J. Geophys. Res.* **109** doi:10.1029/2003JC001788
[28] Kawai S *et al* 1977 *J. Oceanogr. Soc. Japan* **33** 137
[29] Forristall G Z 1981 *J. Geophys. Res.* **86** 8075
[30] Mitsuyasu H *et al* 1980 *J. Phys. Oceanogr.* **10** 286
[31] Wilson B W 1965 *Dt. Hydrogr. Z.* **18** 114
[32] Lamb H 1932 *Hydrodynamics* 6th ed. (Cambridge: Cambridge University Press)